Metal–Organic Frameworks

Deutsche Ausgabe: DOI: 10.1002/ange.201501691
Internationale Ausgabe: DOI: 10.1002/anie.201501691

Postsynthetic Improvement of the Physical Properties in a Metal–Organic Framework through a Single Crystal to Single Crystal Transmetallation**

Thais Grancha, Jesús Ferrando-Soria, Hong-Cai Zhou, Jorge Gascon,* Beatriz Seoane, Jorge Pasán, Oscar Fabelo, Miguel Julve, and Emilio Pardo**

In memory of Olivier Kahn

Abstract: *A single crystal to single crystal transmetallation process takes place in the three-dimensional (3D) metal–organic framework (MOF) of formula $Mg^{II}_2\{Mg^{II}_4[Cu^{II}_2(Me_3mpba)_2]_3\}\cdot 45\,H_2O$ (**1**; Me_3mpba^{4-} = N,N′-2,4,6-trimethyl-1,3-phenylenebis(oxamate)). After complete replacement of the Mg^{II} ions within the coordination network and those hosted in the channels by either Co^{II} or Ni^{II} ions, **1** is transmetallated to yield two novel MOFs of formulae $Co^{II}_2\{Co^{II}_4[Cu^{II}_2(Me_3mpba)_2]_3\}\cdot 56\,H_2O$ (**2**) and $Ni^{II}_2\{Ni^{II}_4[Cu^{II}_2(Me_3mpba)_2]_3\}\cdot 54\,H_2O$ (**3**). This unique postsynthetic metal substitution affords materials with higher structural stability leading to enhanced gas sorption and magnetic properties.*

The design and synthesis of metal–organic frameworks (MOFs) have experienced a rapid development during the past years.[1] Since the pioneering works on the structural chemistry of MOFs,[2] interest in this field has increased exponentially. In addition to the wide range of physical and chemical properties that MOFs can exhibit,[3] this unique class of molecular multifunctional materials provide an excellent playground to study complex supramolecular dynamic processes.[4]

An accurate control of the MOF structure through ligand design is crucial to achieve the desired properties. In this sense, MOFs with predetermined dimensionalities and specific topologies can be designed, to a certain extent, by a careful choice of metal ions and organic ligands. However, a total control of the MOF structure is not always possible because of the many subtle factors that may affect their assembly.[5] Alternative synthetic routes for the synthesis of MOFs with the desired physical properties, consisting of ligand chemical modification and/or metal substitution (transmetallation) of a preformed MOF without altering its structure, are very promising because of the possibility to better control the nature of the ligand spacers and the interacting metal nodes of the MOF structure.[6] Up to now, only a few examples showing a complete transmetallation within the coordination network of the MOF have been reported, with partial transmetallation within the pores being more frequently observed.[7] This is not surprising considering that controlling selective bond destruction and formation in the solid state has proved challenging.

Herein, we report a unique solid-state transmetallation in a new series of oxamato-based 3D MOFs with two exchangeable metal sites of general formula $M^{II}_2\{M^{II}_4[Cu^{II}_2(Me_3mpba)_2]_3\}\cdot n\,H_2O$ (**1**: M = Mg, $n = 45$; **2**: M = Co, $n = 56$; **3**: M = Ni, $n = 54$) where Me_3mpba^{4-} is the *N*,*N*′-2,4,6-trimethyl-1,3-phenylenebis(oxamate) ligand. Interestingly, the reported postsynthetic ion-exchange process is reflected in a significant improvement of the structural stability and the gas sorption and magnetic properties of the original precursor (**1**) to afford two novel examples of porous magnets (**2** and **3**) of the bimetallic oxamate family.[8]

1 was obtained as brownish green prisms by the direct reaction of aqueous solutions of the dicopper(II) complex $Na_4[Cu_2(Me_3mpba)_2]\cdot 4\,H_2O$[8b] and $Mg(NO_3)_2\cdot 4\,H_2O$ (1:2

[*] T. Grancha, Prof. Dr. M. Julve, Dr. E. Pardo
Instituto de Ciencia Molecular (ICMOL), Universitat de València
Paterna 46980, València (Spain)
E-mail: emilio.pardo@uv.es
Dr. J. Ferrando-Soria, Prof. Dr. H.-C. Zhou
Department of Chemistry, Texas A&M University
College Station, TX 77842-3012 (USA)
E-mail: jesus.ferrando@uv.es
Prof. Dr. J. Gascon, Dr. B. Seoane
Catalysis Engineering-Chemical Engineering Department
Delft University of Technology
Julianalaan 136, 2628 BL Delft (The Netherlands)
E-mail: j.gascon@tudelft.nl
Dr. J. Pasán
Laboratorio de Rayos X y Materiales Moleculares
Departamento de Física, Universidad de La Laguna
La Laguna 38201, Tenerife (Spain)
Dr. O. Fabelo
Institut Laue Langevin, Diffraction Group
Grenoble 38042 (France)

[**] This work was supported by the MINECO (Spain) (Projects CTQ2013-46362-P and CTQ2013-44844-P) and the Generalitat Valenciana (Spain) (Project PROMETEOII/2014/070). B.S. and J.G. acknowledge the financial support of the European Research Council under the European Union's Seventh Framework Programme (FP/2007-2013)/ERC Grant Agreement no. 335746, CrystEng-MOF-MMM. T.G. thanks the Universitat de València for a predoctoral contract. We acknowledge SOLEIL for provision of synchrotron radiation facilities and we would like to thank Pierre Fertey for assistance in using beamline CRISTAL. Thanks are also extended to the Ramón y Cajal Program (E.P.).

Supporting information for this article is available on the WWW under http://dx.doi.org/10.1002/anie.201501691.

molar ratio) at room temperature by slow diffusion in a H-shaped tube. **2** and **3** were obtained through a double cation-exchange reaction in the solid state by immersing crystals of **1** in saturated aqueous solutions of $M(NO_3)_2{\cdot}6H_2O$ (M = Co (**2**), Ni (**3**)) for several weeks. The whole exchange process was followed visually and no crystal dissolution was observed. Moreover, the final crystals had the same size and shape as those of the original ones. These facts rule out a possible dissolution–recrystallization mechanism for this system, and strongly suggest a solid-state process.[6d] The crystal structures of **1**–**3** could be determined by single-crystal X-ray diffraction using synchrotron radiation at the CRISTAL beamline in the Synchrotron SOLEIL (see Experimental Section, Supporting Information).

1–**3** crystallize in the same *P*4/*mmm* space group of the tetragonal system (see Table S1 in the Supporting Information). All three isostructural compounds consist of anionic 3D $M^{II}{}_4Cu^{II}{}_6$ (M = Mg (**1**), Co (**2**), Ni (**3**)) open-framework structures with hydrated M^{II} countercations occupying their cavities together with a varying amount of crystallization water molecules. The anionic 3D network of **1**–**3** can be described as an extended parallel array of oxamato-bridged $M^{II}{}_4Cu^{II}{}_6$ layers growing in the *ab* plane with a mixed square/octagonal ($4{\cdot}8^2$) net topology (Figure 1 and Figure S1). The layers are further interconnected through the two trimethyl-substituted *m*-phenylene spacers among the Cu^{II} ions, as earlier found in the related manganese(II) derivative of formula $Na^{I}{}_4\{Mn^{II}{}_4[Cu^{II}{}_2(Me_3mpba)_2]_3\}{\cdot}60H_2O$.[8b]

These features yield a common porous structure for **1**–**3** with a trimodal pore-size distribution along the *c* axis made up of one single type of square pores but two types of octagonal pores (Figure 1). These two types of octagonal pores result from the distinct orientation of the trimethyl-substituted phenylene spacers pointing into or out from the channels, which is reflected in their relative diameters of circa 1.5 and 2.0 nm. However, the occupation of the channels by the corresponding countercations is very different for the starting compound **1** and the transmetallated species **2** and **3**. In **1**, the hydrated Mg^{II} counterions are alternatively located in both the narrow and wide octagonal channels: half of them (Mg2) are weakly bound to the carboxylate oxygen atoms from the anionic network, whereas the remaining half (Mg3) are hydrogen bonded through the coordinated water molecules to the anionic network (Figure 1a and Figure S2a). In contrast, for **2** and **3**, the hydrated M^{II} counterions coming from the metal-ion-exchange process (M = Co (**2**), Ni (**3**)) can only be found in the largest octagonal channels (being hydrogen bonded to the coordination network) but also in the small square ones (Figure 1b and Figure S2b). The estimated values of the empty volume without the crystallization water molecules are 11074 (**1**), 11073 (**2**), and 11023 Å^3 (**3**), which represent up to circa 54.7 (**1**), 54.8 (**2**), and 55.4% (**3**) of potential empty space per unit cell volume (V = 20262 (**1**), 20216 (**2**), and 19911 Å^3 (**3**)).

To elucidate the mechanism of the transmetallation process, we monitored the exchange of Mg^{II} ions in **1** by M^{II} ions (M = Co (**2**), Ni (**3**)) through inductively coupled plasma atomic absorption spectroscopy (ICP-AES) and SEM using single crystals (Figure S3 and Figure 2). First aiming at clarifying the thermodynamics of metal-ion exchange, we studied the variation in metal stoichiometry within the MOF (Mg^{II}:Cu^{II} and M^{II}:Cu^{II}) at different M^{II} concentrations and long exchange times (14 days). Figure S3 reveals essentially the same ion-exchange pathway consisting of a continuous decrease of the Mg^{II} occupancy (and a concomitant increase of the M^{II} occupancy) with increasing [M^{II}] up to reaching saturation (at lower M^{II} concentrations for M = Co than for M = Ni). This overall behavior suggests a rather similar thermodynamic stability for both metal sites, that is, for those within the channels and those of the coordination

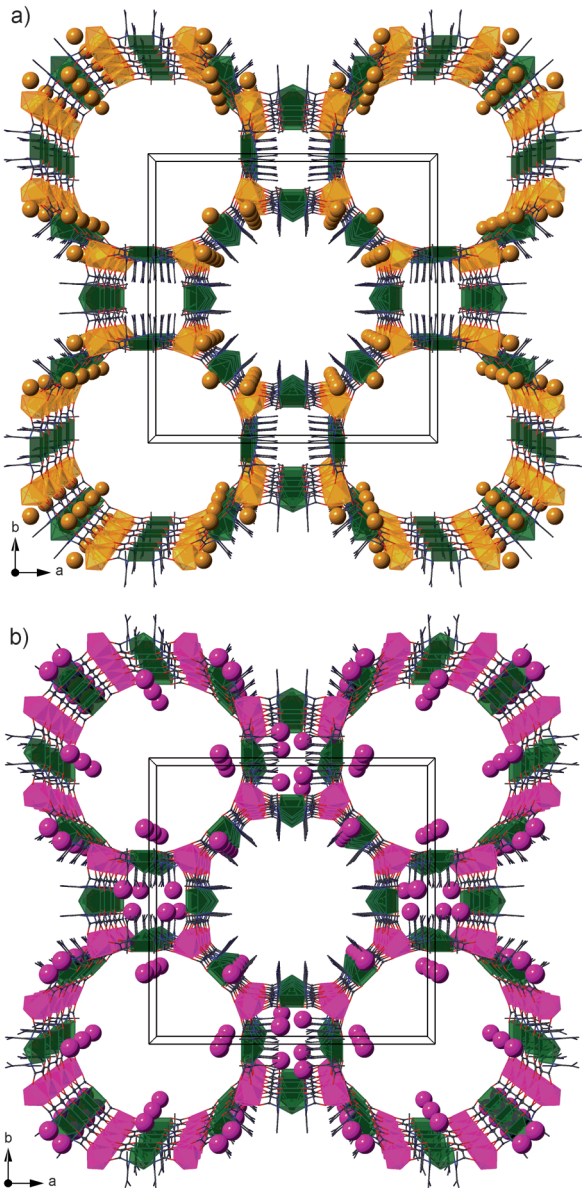

Figure 1. Perspective views of the anionic 3D $M^{II}{}_4Cu^{II}{}_6$ networks of a) **1** and b) **2**/**3** along the crystallographic *c* axis, showing the different site occupation of the channels by the M^{II} countercations (the coordinated and crystallization H_2O molecules are omitted for clarity). Polyhedra represent atoms in the coordination network and spheres represent atoms occupying the channels. Polyhedra colors: Cu = green; Mg = orange; Co/Ni = purple. Sphere colors: Mg = orange; Co/Ni = purple.

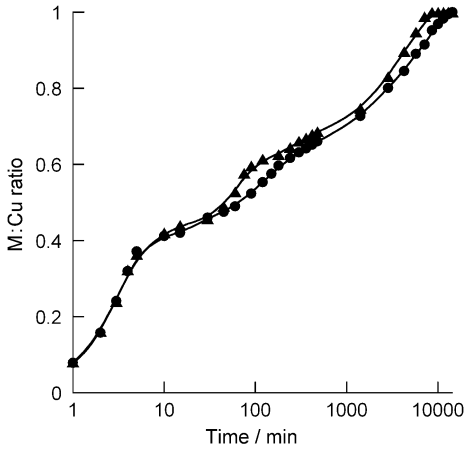

Figure 2. Kinetic profile of the ion exchange represented as the M^{II}:Cu^{II} ratio (M^{II} = Co^{II} (▲), Ni^{II} (●)) versus time plot (in semilogarithmic scale).

network. Second, the kinetics of the metal-ion exchange were monitored through the increase of the M^{II}:Cu^{II} ratio within the MOF, which was measured at specific time intervals (0–10 days) of immersion of the solid in saturated M^{II} aqueous solutions (Figure 2). A very fast exchange of around two out of six Mg^{II} ions takes place (in less than 5 min of exposure). This identical behavior for both Co^{II} and Ni^{II} substitutions, together with reaching the same M^{II}:Cu^{II} ratio, strongly suggest that this first step corresponds to the substitution of those metal ions hosted in pores. Afterwards, a slower substitution of the remaining four Mg^{II} ions by M^{II} ions takes place over the course of five (M = Co) and seven days (M = Ni), respectively, leading to complete transmetallation of the network. Interestingly, an intermediate saturation step (more obvious in the case of the Co^{II} derivative) can be observed at a M^{II}:Cu^{II} ratio of around 0.66 (Figure 2), which is likely related to cooperative effects in the occupation of the coordination network. These thermodynamic and kinetic results suggest an associative mechanism involved in the ion-exchange process.[6c] Additionally, the presence of weakly coordinated magnesium ions hosted in the channels (see structural section above) also supports that the Mg^{II} ions from the coordination network are replaced by those M^{II} ions previously situated in the channels located in close proximity to them. Preliminary studies suggest that the exchange process is reversible.

The powder X-ray diffraction (PXRD) patterns of freshly prepared samples of **1**–**3** (prepared from suspensions in water) are almost identical and they are consistent with the calculated ones (Figure S4). The correspondence of experimental and calculated structures confirms that the bulk samples are isostructural to the crystals selected for single-crystal X-ray diffraction, and that the open-framework structures remain unchanged after the transmetallation reaction. The water contents of **1**–**3** were independently determined by thermogravimetric analysis (TGA) under a dry N_2 atmosphere (Figure S5). All three compounds present a qualitatively similar behavior with a fast mass loss from room temperature followed by a "plateau" in the mass loss until decomposition begins. The estimated percentage weight loss values of 26 (**1**), 29 (**2**), and 28% (**3**) at 130°C correspond to circa 45 (**1**), 56 (**2**), and 54 (**3**) water molecules, respectively.

To check the structural stability of the MOF structure upon removal of water molecules, variable-temperature PXRD studies were also carried out at 25, 70, 80, and 97°C for **1**–**3** (Figure S6). **1** loses crystallinity very fast once removed from the water solution and further deteriorates when heating. Thus, its activated (dehydrated) phase shows a very poor crystallinity, suggesting a complete collapse of the open-framework structure of the original hydrated phase upon solvent removal (Figure S6a). **2** also loses crystallinity when exposed to air but the intensity of the peaks do not appreciably decrease when heated to 97°C (Figure S6b). In contrast, the variable-temperature PXRD patterns of **3** show well-resolved peaks, which are located at the same positions and with similar intensities to those of the original hydrated phase, confirming the robustness of the MOF upon solvent removal (Figure S6c).

These PXRD results suggest that very different gas sorption properties should be observed for compounds **1**–**3**, as depicted by Figure 3. The N_2 adsorption isotherms at 77 K of **1**–**3** show a type I sorption behavior characteristic of microporous compounds (Figure 3a). The sorption capacities for each compound follow the trend **1** < **2** < **3**, as expected from the variable-temperature PXRD studies, with estimated Brunauer–Emmett–Teller (BET) surface areas of 444 (**1**), 613 (**2**), and 905 $m^2 g^{-1}$ (**3**).

To further confirm the effect of the metal-atom substitution on their gas sorption capacities, we also measured high-

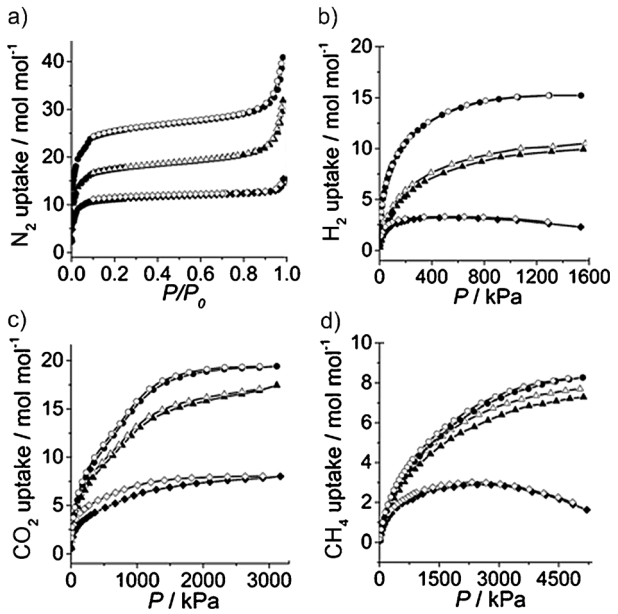

Figure 3. a) Low-pressure N_2 (77 K) and high-pressure b) H_2 (77 K), c) CO_2 (273 K), and d) CH_4 (273 K) sorption isotherms for the activated compounds **1** (◆), **2** (▲), and **3** (●). Filled and empty symbols indicate the adsorption and desorption isotherms, respectively. In (a–d), **1** is the bottom curve, **2** appears in the middle, and **3** at the top. Sorption units given in mol of adsorbate per mol of dehydrated MOF.

pressure H_2 (77 K), CO_2 (273 K), and CH_4 (273 K) adsorption isotherms of **1**–**3** (Figure 3b–d). Overall, a significant increase of the sorption capacities can be observed for the transmetallated species **2** and **3** (with a larger increase for Ni^{II} derivative **3**). The greater sorption capacity of **2** and especially **3** can be attributed both to the larger ion–quadrupole interactions because of the presence of Co^{II} and Ni^{II} ions and to the aforementioned increase of the structural stability in **2** and, more remarkably, in **3**. Although the gas uptakes follow, for all of the gases, the general trend **1** < **2** < **3**, the **2**:**1** and **3**:**1** adsorption ratios are quite different depending on the measured gas. These results suggest that this postsynthetic method for the preparation of MOFs is not only able to improve the adsorption capacity of a given material but also to tune its gas selectivity, opening the door for "à la carte" postsynthetic rational syntheses depending on the gases that should be separated.

The magnetic behavior of **1**–**3** was investigated through magnetic susceptibility measurements in both direct- (dc) and alternating-current (ac) fields. As expected, the exchange of the diamagnetic Mg^{II} ions (**1**) by paramagnetic Co^{II} (**2**) and Ni^{II} ions (**3**) (with $S_{Co} = 3/2$ and $S_{Ni} = 1$) has a dramatic influence in their dc magnetic properties (Figure S7). **1** behaves as well-isolated ferromagnetically coupled dicopper(II) units with a moderate ferromagnetic coupling between the two Cu^{II} ions. The Cu^{II} ions are coupled through the trimethyl-substituted phenylenediamidate bridges (with coupling constant $J = +14.0\ cm^{-1}$; this was fit using the Hamiltonian $H = -JS_1S_2$ with $S_1 = S_2 = S_{Cu} = 1/2$; solid line in the inset of Figure S7a).[9] In contrast, **2** and **3** show a typical ferrimagnetic behavior resulting from the strong antiferromagnetic coupling between the Cu^{II} and M^{II} ions through the oxamato bridge within each $M^{II}_4Cu^{II}_6$ layer (M = Co (**2**), Ni (**3**)), as previously found in the related manganese(II) derivative.[8b]

These overall ferro- (**1**) and ferrimagnetic (**2**, **3**) behaviors are further confirmed by the magnetization per formula unit (M) versus applied dc magnetic field (H) plots at 2.0 K (Figure S8). More importantly, a magnetic hysteresis loop is measured for both **2** and **3** at 2.0 K, with values of the coercive field of $H_c = 150$ (**2**) and 300 G (**3**) which are typical of soft magnets (inset of Figure S8).

The occurrence of a long-range 3D magnetic ordering in **2** and **3** is evidenced by the presence of a sharp frequency-independent maximum in the χ_M'' versus T plots (χ_M'' being the out-of-phase ac molar magnetic susceptibility per formula unit) at critical temperatures of $T_C = 22.5$ (**2**) and 25.0 K (**3**) (Figure 4). This is further confirmed by the M versus T plots (inset, Figure 4), which show an abrupt increase below circa 22.5 (**2**) and 25.0 K (**3**). These T_C values are somewhat higher than that earlier reported for the manganese(II) derivative ($T_C = 21.0$ K).[8b] Overall, this indicates that there exists an effective ferromagnetic interaction between the oxamato-bridged $M^{II}_4Cu^{II}_6$ ferrimagnetic layers. This interaction results from the weak ferromagnetic coupling between the Cu^{II} ions across the double 2,4,6-trimethyl-phenylenediamidate bridge within the Cu^{II}_2 pillaring units, as revealed by the magnetic behavior of **1**. Besides these "through-bond" interlayer interactions, the dipolar interactions with the paramagnetic

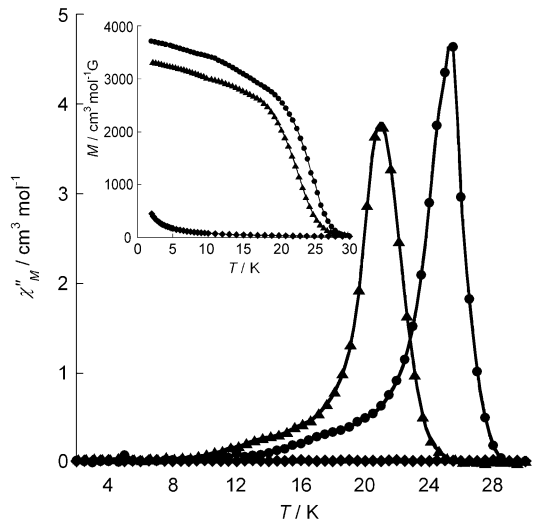

Figure 4. Temperature dependence of the ac current out-of-phase molar magnetic susceptibility (χ_M'') of **1** (◆), **2** (▲), and **3** (●) with a ±4.0 G field oscillating at 1000 Hz. Inset: temperature dependence of the magnetization (M) of **1** (◆), **2** (▲), and **3** (●).

high-spin M^{II} ions (M = Co (**2**), Ni (**3**)) hosted in the channels of the MOF may also play a non-negligible role on the long-range 3D magnetic ordering. This idea is supported by the higher T_C values of **2** and **3** when compared to the related manganese(II) derivative with diamagnetic sodium(I) ions as cationic hosts.[8b]

In summary, **1** exhibits a complete exchange of the Mg^{II} ions hosted in the channels and those constituting the heterobimetallic network after immersion in saturated aqueous Ni^{II} and Co^{II} solutions to afford **2** and **3**. Both the structural integrity of the framework and the crystallinity are maintained upon transmetalation of **1** to form **2** or **3**. Although the exchange of the metal counterions hosted in the channels has been observed previously in several MOFs acting as ion exchangers,[10] the reported exchange of the metal centers constituting the coordination framework has been rarely observed[7] and, in some cases, just in a partial manner.[11] More importantly, the postsynthetic transmetallation process of **1** affords materials with enhanced structural stability (which is especially relevant for **3**), as shown by a drastic improvement of the gas sorption properties. Finally, the substitution of the diamagnetic Mg^{II} ions in **1** by paramagnetic Ni^{II} and Co^{II} ions is responsible for the occurrence of a long-range magnetic ordering in **2** and **3**. Attempts to synthesize compounds **2** and **3** directly using slow diffusion methods were unsuccessful. These results demonstrate the clear advantages of postsynthetic methods to obtain MOFs with rationally predetermined architectures as well as improved, or even new, physical properties.

Keywords: gas sorption · magnetic properties · metal–organic frameworks · transmetalation · X-ray diffraction

How to cite: *Angew. Chem. Int. Ed.* **2015**, *54*, 6521–6525
Angew. Chem. **2015**, *127*, 6621–6625

[1] a) N. L. Rosi, M. Eddaoudi, J. Kim, M. O'Keeffe, O. M. Yaghi, *CrystEngComm* **2002**, *4*, 401 – 404; b) C. Janiak, *Dalton Trans.* **2003**, 2781 – 2804; c) D. Bradshaw, J. B. Claridge, E. J. Cussen, T. J. Prior, M. J. Rosseinsky, *Acc. Chem. Res.* **2005**, *38*, 273 – 282; d) S. Kitagawa, R. Matsuda, *Coord. Chem. Rev.* **2007**, *251*, 2490 – 2509; e) G. Férey, *Chem. Soc. Rev.* **2008**, *37*, 191 – 214; f) J. R. Long, O. M. Yaghi, *Chem. Soc. Rev.* **2009**, *38*, 1213 – 1214.

[2] a) B. F. Abrahams, B. F. Hoskins, D. M. Michail, R. Robson, *Nature* **1994**, *369*, 727 – 729; b) S. R. Batten, R. Robson, *Angew. Chem. Int. Ed.* **1998**, *37*, 1460 – 1494; *Angew. Chem.* **1998**, *110*, 1558 – 1595.

[3] a) D. Maspoch, D. Ruiz-Molina, J. Veciana, *Chem. Soc. Rev.* **2007**, *36*, 770 – 818; b) P. Dechambenoit, J. R. Long, *Chem. Soc. Rev.* **2011**, *40*, 3249 – 3265; c) E. Coronado, J. R. Galán-Mascarós, C. J. Gómez-García, V. Laukhin, *Nature* **2000**, *408*, 447 – 449; d) E. Pardo, C. Train, G. Gontard, K. Boubekeur, O. Fabelo, H. Liu, B. Dkhil, F. Lloret, K. Nakagawa, H. Tokoro, S.-I. Ohkoshi, M. Verdaguer, *J. Am. Chem. Soc.* **2011**, *133*, 15328 – 15331; e) G.-C. Xu, W. Zhang, X.-M. Ma, Y.-H. Chen, L. Zhang, H.-L. Cai, Z.-M. Wang, R.-G. Xiong, S. Gao, *J. Am. Chem. Soc.* **2011**, *133*, 14948 – 14951; f) E. Pardo, C. Train, H. Liu, L.-M. Chamoreau, B. Dkhil, K. Boubekeur, F. Lloret, K. Nakatani, H. Tokoro, S.-I. Ohkoshi, M. Verdaguer, *Angew. Chem. Int. Ed.* **2012**, *51*, 8356 – 8360; *Angew. Chem.* **2012**, *124*, 8481 – 8485; g) S.-I. Ohkoshi, K. Imoto, Y. Tsunobuchi, S. Takano, H. Tokoro, *Nat. Chem.* **2011**, *3*, 564 – 569; h) L. E. Kreno, K. Leong, O. K. Farha, M. Allendorf, R. P. Van Duyne, J. T. Hupp, *Chem. Rev.* **2012**, *112*, 1105 – 1125; i) C. Train, M. Gruselle, M. Verdaguer, *Chem. Soc. Rev.* **2011**, *40*, 3297 – 3312; j) C. Train, R. Gheorghe, V. Krstic, L.-M. Chamoreau, N. S. Ovanesyan, G. L. J. Rikken, M. Gruselle, M. Verdaguer, *Nat. Mater.* **2008**, *7*, 729 – 734.

[4] a) O. M. Yaghi, M. O'Keeffe, N. W. Ockwig, H. K. Chae, M. Eddaoudi, J. Kim, *Nature* **2003**, *423*, 705 – 714; b) J.-R. Li, R. J. Kuppler, H.-C. Zhou, *Chem. Soc. Rev.* **2009**, *38*, 1477 – 1504.

[5] M. G. Goesten, F. Kapteijn, J. Gascon, *CrystEngComm* **2013**, *15*, 9249 – 9257.

[6] a) S. M. Cohen, *Chem. Rev.* **2012**, *112*, 970 – 1000; b) M. Lalonde, W. Bury, O. Karagiaridi, Z. Brown, J. T. Hupp, O. K. Farha, *J. Mater. Chem. A* **2013**, *1*, 5453 – 5468; c) C. K. Brozek, M. Dincă, *Chem. Soc. Rev.* **2014**, *43*, 5456 – 5467; d) X. Cui, A. N. Khlobystov, X. Chen, D. H. Marsh, A. J. Blake, W. Lewis, N. R. Champness, C. J. Roberts, M. Schröder, *Chem. Eur. J.* **2009**, *15*, 8861 – 8873.

[7] a) S. Das, H. Kim, K. Kim, *J. Am. Chem. Soc.* **2009**, *131*, 3814 – 3815; b) Y. Kim, S. Das, S. Bhattacharya, S. Hong, M. G. Kim, M. Yoon, S. Natarajan, K. Kim, *Chem. Eur. J.* **2012**, *18*, 16642 – 16648; c) G. Mukherjee, K. Biradha, *Chem. Commun.* **2012**, *48*, 4293 – 4295; d) X.-J. Wang, P.-Z. Li, L. Liu, Q. Zhang, P. Borah, J. D. Wong, X. X. Chan, G. Rakesh, Y. Li, Y. Zhao, *Chem. Commun.* **2012**, *48*, 10286 – 10288; e) Z. Zhang, L. Zhang, L. Wojtas, P. Nugent, M. Eddaoudi, M. J. Zaworotko, *J. Am. Chem. Soc.* **2012**, *134*, 924 – 927; f) T.-F. Liu, L. Zou, D. Feng, Y.-P. Chen, S. Fordham, X. Wang, Y. Liu, H.-C. Zhou, *J. Am. Chem. Soc.* **2014**, *136*, 3 – 6.

[8] a) J. Ferrando-Soria, J. Pasán, C. Ruiz-Pérez, Y. Journaux, M. Julve, F. Lloret, J. Cano, E. Pardo, *Inorg. Chem.* **2011**, *50*, 8694 – 8696; b) J. Ferrando-Soria, P. Serra-Crespo, M. de Lange, J. Gascon, F. Kapteijn, M. Julve, J. Cano, F. Lloret, J. Pasán, C. Ruiz-Pérez, Y. Journaux, E. Pardo, *J. Am. Chem. Soc.* **2012**, *134*, 15301 – 15304; c) J. Ferrando-Soria, T. Grancha, M. Julve, J. Cano, F. Lloret, Y. Journaux, J. Pasán, C. Ruiz-Pérez, E. Pardo, *Chem. Commun.* **2012**, *48*, 3539 – 3541; d) J. Ferrando-Soria, T. Grancha, J. Pasán, C. Ruiz-Pérez, L. Cañadillas-Delgado, Y. Journaux, M. Julve, J. Cano, F. Lloret, E. Pardo, *Inorg. Chem.* **2012**, *51*, 7019 – 7021; e) J. Ferrando-Soria, H. Khajavi, P. Serra-Crespo, J. Gascon, F. Kapteijn, M. Julve, F. Lloret, J. Pasán, C. Ruiz-Pérez, Y. Journaux, E. Pardo, *Adv. Mater.* **2012**, *24*, 5625 – 5629; f) J. Ferrando-Soria, M. T. M. Rood, M. Julve, F. Lloret, Y. Journaux, J. Pasán, C. Ruiz-Pérez, O. Fabelo, E. Pardo, *CrystEngComm* **2012**, *14*, 761 – 764; g) J. Ferrando-Soria, R. Ruiz-García, J. Cano, S.-E. Stiriba, J. Vallejo, I. Castro, M. Julve, F. Lloret, P. Amorós, J. Pasán, C. Ruiz-Pérez, Y. Journaux, E. Pardo, *Chem. Eur. J.* **2012**, *18*, 1608 – 1617; h) T. Grancha, C. Tourbillon, J. Ferrando-Soria, M. Julve, F. Lloret, J. Pasán, C. Ruiz-Pérez, O. Fabelo, E. Pardo, *CrystEngComm* **2013**, *15*, 9312 – 9315.

[9] I. Fernández, R. Ruiz, J. Faus, M. Julve, F. Lloret, J. Cano, X. Ottenwaelder, Y. Journaux, M. C. Muñoz, *Angew. Chem. Int. Ed.* **2001**, *40*, 3039 – 3042; *Angew. Chem.* **2001**, *113*, 3129 – 3132.

[10] a) D. Denysenko, T. Werner, M. Grzywa, A. Puls, V. Hagen, G. Eickerling, J. Jelic, K. Reuter, D. Volkmer, *Chem. Commun.* **2012**, *48*, 1236 – 1238; b) T. Jacobs, R. Clowes, A. I. Cooper, M. J. Hardie, *Angew. Chem. Int. Ed.* **2012**, *51*, 5192 – 5195; *Angew. Chem.* **2012**, *124*, 5282 – 5285; c) R. Yao, X. Xu, X. Zhang, *Chem. Mater.* **2012**, *24*, 303 – 310.

[11] a) M. Kim, J. F. Cahill, H. Fei, K. Prather, S. M. Cohen, *J. Am. Chem. Soc.* **2012**, *134*, 18082 – 18088; b) C. K. Brozek, M. Dincă, *J. Am. Chem. Soc.* **2013**, *135*, 12886 – 12891; c) H. Fei, J. F. Cahill, K. Prather, S. M. Cohen, *Inorg. Chem.* **2013**, *52*, 4011 – 4016; d) M. Dincă, J. R. Long, *J. Am. Chem. Soc.* **2007**, *129*, 11172 – 11176; e) Z.-J. Zhang, W. Shi, Z. Niu, H.-H. Li, B. Zhao, P. Cheng, D.-Z. Liao, S.-P. Yan, *Chem. Commun.* **2011**, *47*, 6425 – 6427.

Received: February 21, 2015
Published online: April 14, 2015

